CYBERNETICS AND PHYSICS, VOL. 14, NO. 3, 2025, 285–291

PDE-CONSTRAINED OPTIMAL CONTROL OF SUBSURFACE RESERVOIR SYSTEMS VIA NEURAL OPERATOR SURROGATES

Daniil Sirota
Saint Petersburg State University
Russian Federation
ds11011@yandex.ru

Dmitri Ovsyannikov
Saint Petersburg State University
Russian Federation
dovs45@mail.ru

Article history:
Received 22.09.2025, Accepted 20.11.2025

Abstract

This paper presents a neural operator-based approach to solving optimal control problems for subsurface reservoir systems. Reservoirs are complex distributed-parameter systems governed by partial differential equations (PDEs). Conventional approaches that solve the governing equations numerically provide high-fidelity simulations of transient flow in porous media but are computationally intensive: for many scenarios, runtimes reach hours even on high-performance computing (HPC) clusters. Consequently, computational efficiency is a key bottleneck for deploying numerical reservoir simulators in decision support and optimal control.

Modern deep learning methods—specifically, neural operators trained on reservoir simulation data—offer a fast and effective alternative for approximating PDE solution operators. Owing to their differentiable structure, neural operators support automatic differentiation of objective functionals, enabling gradient-based optimization with substantially reduced computational cost.

The main contributions are a theoretical upper bound on the control error that depends explicitly on properties of the neural operator, and the development of an optimal control method within the proposed framework. Practical relevance and high computational efficiency are demonstrated on a reservoir well-control optimization problem, illustrating the method's applicability to real-field settings that demand fast evaluation of operational strategies and consistent enforcement of production constraints.

Key words

Optimal control, oil and gas reservoirs, neural operators, flow in porous media.

1 Introduction

In this work, we consider subsurface reservoirs as distributed-parameter systems. These are geological formations—specifically, porous media saturated with oil, gas, or water—that are subject to physical fields [Aziz and Settari, 1979]. The system dynamics, driven by interactions among formations, wells, and fluids, are governed by partial differential equations (PDEs) of transient flow in porous media.

The optimal control of such systems is formulated as a PDE-constrained optimization problem: minimizing an objective functional, which typically reflects operational or economic criteria, subject to constraints on both the control parameters (e.g., well flow rates) and the state variables (e.g., pressure or saturation fields) [Lurie, 1993; Lions, 1971; Hinze, 2009]. Such optimization challenges are ubiquitous across the energy value chain, extending from subsurface flows in porous media [Zakirov et al., 1996] to downstream separation processes [Arguchintsev and Kopylov, 2023; Arguchintsev and Kopylov, 2024]. A cornerstone technique for solving such problems is the adjoint method, which provides an efficient means of computing the gradient of the objective functional with respect to the controls. The computational cost of this method is notably independent of the number of control parameters, making it highly effective for large-scale applications [Sarma et al., 2006; Jansen, 2011; Kourounis et al., 2014].

High-fidelity mathematical models are central to any optimal control strategy for reservoir systems, as they are essential for predicting system response to control actions. However, classical numerical methods widely employed in reservoir simulators (e.g., the finite volume method for spatial discretization coupled with an implicit Euler scheme for time integration) incur substantial computational costs. This high computational complexity severely limits their practicality for real-time control of processes such as oil and gas production, underground gas storage (UGS) operations, and carbon dioxide (CO_2) sequestration.

To overcome the significant computational cost of classical schemes like the finite volume method, machine learning surrogates are increasingly integrated directly into numerical solvers to accelerate expensive physics calculations, as demonstrated in high-speed gas dynamics [Istomin and Pavlov, 2023]. Building on this trend to address the limitations of traditional modeling in subsurface flows, this work employs neural operators as efficient surrogates for the governing PDEs. Grounded in universal approximation theorems, neural operators are a class of deep learning models specifically designed to approximate nonlinear operators between infinite-dimensional function spaces [Lu et al., 2021; Kovachki et al., 2023; Li et al., 2020]. This fundamentally distinguishes them from standard neural network architectures, which operate on finite-dimensional spaces. A key advantage of neural operators is their ability, once trained on a limited dataset, to approximate the PDE solution operator while maintaining discretization invariance. A well-trained operator can accurately predict solutions for varying reservoir geometries, initial and boundary conditions, and fluid/rock properties without the need for retraining.

The objective of this work is to develop an optimal control framework for reservoir systems that leverages a trained neural operator as a surrogate model and to establish a theoretical upper bound on the resulting control error.

2 Model of subsurface flow in porous media

In this work we employ a Fourier Neural Operator modified for optimization (TFNO-opt) with four layers. The detailed problem setup, as well as the architecture design and training procedures for reservoir simulation tasks, are described in [Sirota et al., 2024; Sirota et al., 2025]. The TFNO-opt model is designed to approximate the PDEs governing three-dimensional transient gas flow in porous media. With homogeneous Neumann (no-flow) boundary conditions and a prescribed initial pressure field, the governing equation can be written in the following form [Ertekin et al., 2001, p. 68]:

$$\nabla\cdot\left(\frac{A\mathbf{k}}{\mu_g B_g}\nabla p\right)\Delta\mathbf{x} = \frac{V_b\phi T_{sc}}{p_{sc}T_{res}}\frac{\partial}{\partial t}\left(\frac{p}{Z}\right) - q \text{ in } \Omega\times(0,T],$$
$$\partial_n p\big|_{\partial\Omega} = 0, \quad p(\cdot,0) = p_0, \tag{1}$$

where p denotes pressure, q is the gas flow rate at standard conditions, $\nabla = \left(\frac{\partial}{\partial x}, \frac{\partial}{\partial y}, \frac{\partial}{\partial z}\right)$ is the gradient operator, $\mathbf{k} = (k_x, k_y, k_z)$ is the (diagonal) permeability tensor, $A = (A_x, A_y, A_z)$ are cross-sectional areas along the coordinate axes, $\Delta\mathbf{x} = (\Delta x, \Delta y, \Delta z)$ is the vector of control volume dimensions, $B_g = \frac{p_{\text{sc}}TZ}{T_{\text{sc}}p}$ is the gas formation volume factor, Z is the gas compressibility factor (z-factor), μ_g is the gas viscosity, T_{sc} and p_{sc} are temperature and pressure at standard conditions, T_{res} is the reservoir temperature, ϕ is porosity, V_b is the control volume, $\Omega \subset \mathbb{R}^3$ is a bounded open set (the computational domain), $\Gamma = \partial\Omega$ is its Lipschitz boundary, n denotes the outward unit normal, $T > 0$ is the final time, and $p(\cdot, 0)$ is the initial pressure distribution. Equation (1) is solved only numerically and is presented in a form tailored to a finite-volume discretization, which is standard in reservoir modeling.

We adopt standard assumptions for such PDEs [Oleĭnik et al., 1958, p. 693], [Vazquez, 2006, p. 102]: the coefficients in (1) are measurable, bounded, and positive; $0 < p_{\min} \le p \le p_{\max}$; the nonlinear functions $\mu_g(p), B_g(p), Z(p)$ are monotone and Lipschitz continuous; and the permeability tensor $\mathbf{k}$ is uniformly elliptic. Under these conditions, for each $q \in L^2(0,T;L^2(\Omega))$ and $p_0 \in L^2(\Omega)$ there exists a unique weak solution $p \in L^2(0,T;H^1(\Omega)) \cap H^1(0,T;H^{-1}(\Omega))$.

In three-dimensional transient flow, sources and sinks are typically not modeled as distributed, since they are concentrated in wells whose radii are small relative to the reservoir scale [Chen, 2007]. As a simplifying assumption, we consider sources and sinks localized at isolated points $x^{(i)} \in \Omega$. One may then surround each point source/sink by a small sphere excluded from the medium; the surface of this sphere becomes part of the boundary, and the mass flux per unit volume defines the total flow through that surface. A more practical approach is to incorporate point sources and sinks directly into the flow equation [Chen, 2007, p. 67]. In that case, the well model $q \in L^2(0,T;L^2(\Omega))$ takes the form

$$q(t,\mathbf{x}) = \sum_{m=1}^{M_w}\sum_{\nu=1}^{N_m} q_m^{(\nu)}(t)\,\eta_\epsilon\Big(\mathbf{x} - \mathbf{x}_m^{(\nu)}\Big), \tag{2}$$

where $\mathbf{x}_m^{(\nu)} \in \Omega$ are the coordinates of perforation intervals, $q_m^{(\nu)}(t) \in L^2(0,T)$ is the source/sink intensity at perforation ν of well m at time t, $\eta_\epsilon(\mathbf{x}) \in L^2(\Omega)$ is a smooth approximation of the delta function, $\epsilon > 0$, M_w is the number of wells, and N_m is the number of perforations in well m. Wells are assumed not to overlap spatially.

3 Optimal control problem statement

A central goal of this study is to develop a control method for reservoir systems governed by (1), using a trained neural operator as a surrogate for the forward model. Consider the function spaces $U = L^2(0,T;H^1(\Omega)) \cap H^1(0,T;H^{-1}(\Omega))$, $V = L^2(0,T;H^{-1}(\Omega))$, and $Q = L^2(0,T;L^2(\Omega))$, where $\Omega \subset \mathbb{R}^3$ is a bounded open set and $T > 0$ is the final time. The choice of U is natural for parabolic problems, ensuring temporal integrability and appropriate space–time regularity [Lurie, 1993; Lions, 1971] Here $H^{-1}(\Omega)$ denotes the dual of $H^1(\Omega)$.

Let $Q_{ad} \subset L^2(0,T;\mathbb{R}^{M_w})$ be a closed, convex set of admissible controls reflecting operational constraints on wells. In field practice, control is exerted by regulating the rates of a finite number of wells. We represent the controls as the vector of well-rate time profiles:

$$\mathbf{q}(t) = \{q_m(t)\}_{m=1}^{M_w} \in Q_{ad}. \tag{3}$$

Throughout, well rates are nonnegative and bounded, $0 \le q_m(t) \le q_{m,\max}$.

The relation between $\mathbf{q} \in Q_{ad}$ in (3) and the source/sink term $q \in Q$ in the flow equation is determined by (2) and can be written in operator form $\Phi : Q_{ad} \to Q$ as

$$(\Phi\mathbf{q})(t,\mathbf{x}) = \sum_{m=1}^{M_w} q_m(t) \left(\frac{1}{N_m} \sum_{\nu=1}^{N_m} \eta_\epsilon(\mathbf{x} - \mathbf{x}_m^{(\nu)}) \right). \tag{4}$$

Since control is specified per well (not per perforation), (4) distributes each well's rate uniformly across its N_m perforations. Thus Φ maps operational controls (well rates) to the spatially distributed source term in the PDE, yielding $q \in \mathrm{Im}(\Phi) \subset Q$.

Define the pressure drawdown vector $\Delta\mathbf{p}(t)$ as the difference between the average pressure in the near-wellbore region of each well and its bottomhole pressure:

$$\Delta\mathbf{p}(t) = \left\{ \frac{1}{|\omega_m^r|} \int_{\omega_m^r} p(t,\mathbf{x}) d\mathbf{x} - \frac{1}{|\omega_m^{bh}|} \int_{\omega_m^{bh}} p(t,\mathbf{x}) d\mathbf{x} \right\}_{m=1}^{M_w}. \tag{5}$$

Here $\omega_m^r \subset \Omega$ and $\omega_m^{bh} \subset \Omega$ are disjoint subdomains of the near-wellbore region and the bottomhole of well m, respectively.

Let $\psi : \mathbb{R} \to \mathbb{R}$ be a threshold function acting elementwise on the drawdown vector, $\psi(x) = [x - d_*]_+$, where $d_* > 0$ is the critical value of drawdown and $[x]_+ = \max\{x, 0\}$. Define the operator $\Psi : L^2(0,T;\mathbb{R}^{M_w}) \to L^2(0,T;\mathbb{R}^{M_w})$ elementwise by

$$\big(\Psi\Delta\mathbf{p}\big)(t) := \{\psi(\Delta p_m(t))\}_{m=1}^{M_w}.$$

We now state the optimal control problem. Given the operational upper bounds for production well rates $\mathbf{q}_{\max} \in Q_{ad}$, the drawdown threshold $d_* > 0$, and the penalty weight $\lambda > 0$ for exceeding the threshold, we seek controls $\mathbf{q} \in Q_{ad}$ that tend toward the maximum admissible rates while simultaneously minimizing drawdown, subject to the state $p \in U$ solving (1). The objective functional is

$$\begin{aligned} J(p,\mathbf{q}) = &\frac{1}{2} \int_0^T \Big(\mathbf{q}(t) - \mathbf{q}_{\max}(t) \Big)^2 dt \\ &+ \frac{\beta}{2} \int_0^T \Big(\Delta\mathbf{p}(t) \Big)^2 dt + \frac{\lambda}{2} \int_0^T \Big((\Psi\Delta\mathbf{p})(t) \Big)^2 dt, \end{aligned} \tag{6}$$

where $\beta \in \mathbb{R}_+$ is pressure drawdown regularization coefficient and $\lambda \in \mathbb{R}_+$ penalizes threshold exceedance.

The state equation (1) couples $p \in U$ and $q \in Q$ and is written in operator form as $F(p,q) = 0$, where $F : U \times Q \to V$.

Since q is induced by $\mathbf{q} \in Q_{ad}$ via $\Phi : Q_{ad} \to Q$, i.e., $q = \Phi\mathbf{q}$, the control–state relation is given by $F\big(p, \Phi\mathbf{q}\big) = 0$. Let $\mathcal{P} : Q_{ad} \to U$ be the control-to-state (solution) operator [Antil et al., 2018], mapping each control $\mathbf{q} \in Q_{ad}$ to the pressure field $p = \mathcal{P}\mathbf{q} \in U$ that satisfies $F\big(\mathcal{P}\mathbf{q},\ \Phi\mathbf{q}\big) = 0$. Similarly, let $\mathcal{P}_\theta : Q_{ad} \to U$ be the neural operator approximating $\mathcal{P}$.

Assuming the well-posedness of the state equation (1) and that the objective functional J is weakly lower semi-continuous and coercive, the problem admits at least one optimal control $\mathbf{q}^* \in Q_{ad}$ [Lions, 1971].

Passing to the reduced formulation, we eliminate the state by writing $p = \mathcal{P}(\mathbf{q})$. The optimal control problem becomes

$$\min_{\mathbf{q} \in Q_{ad}} \widetilde{J}(\mathbf{q}), \tag{7}$$

where $\widetilde{J}(\mathbf{q}) = J\big(\mathcal{P}\mathbf{q},\ \mathbf{q}\big)$ is the reduced objective.

Define the drawdown operator $\mathcal{D} : U \to L^2(0,T;\mathbb{R}^{M_w})$ acting on the subdomains $\omega_m^r, \omega_m^{bh}$ by

$$\begin{aligned} \Delta\mathbf{p}(t) = &\Bigg\{ \frac{1}{|\omega_m^r|} \int_{\omega_m^r} \big(\mathcal{P}\mathbf{q}\big)(t,\mathbf{x}) d\mathbf{x} \\ &- \frac{1}{|\omega_m^{bh}|} \int_{\omega_m^{bh}} \big(\mathcal{P}\mathbf{q}\big)(t,\mathbf{x})\, d\mathbf{x} \Bigg\}_{m=1}^{M_w}. \end{aligned}$$

Hence,

$$\mathcal{G} = \mathcal{D} \circ \mathcal{P}, \qquad \mathcal{G}_\theta = \mathcal{D} \circ \mathcal{P}_\theta.$$

The reduced objective for the original model reads

$$\begin{aligned} \widetilde{J}(\mathbf{q}) = &\frac{1}{2} \int_0^T \Big(\mathbf{q}(t) - \mathbf{q}_{\max}(t) \Big)^2 dt \\ &+ \frac{\beta}{2} \int_0^T \Big(\mathcal{G}\mathbf{q}(t) \Big)^2 dt + \frac{\lambda}{2} \int_0^T \Big(\Psi(\mathcal{G}\mathbf{q})(t) \Big)^2 dt. \end{aligned} \tag{8}$$

The corresponding reduced objective using the neural operator surrogate is

$$\begin{aligned} \widetilde{J}_n(\mathbf{q}_n) = &\frac{1}{2} \int_0^T \Big(\mathbf{q}_n(t) - \mathbf{q}_{\max}(t) \Big)^2 dt \\ &+ \frac{\beta}{2} \int_0^T \Big(\mathcal{G}_\theta\mathbf{q}_n(t) \Big)^2 dt + \frac{\lambda}{2} \int_0^T \Big(\Psi(\mathcal{G}_\theta\mathbf{q}_n)(t) \Big)^2 dt. \end{aligned} \tag{9}$$

4 Theoretical upper bound for the control error of neural operators

In numerical simulations of flow in reservoir systems, the original nonlinear state equations are typically solved by iterative methods (e.g., Newton-type schemes) that rely on local linearization of the governing equations. In PDE-constrained optimal control, local linearization of the state-to-output operator is a standard tool for analyzing nonlinear systems. Since neural operators are also nonlinear by construction, we analyze the control error and optimality conditions in a neighborhood of the current control iterate $\mathbf{q}^{(k)}$. In such a neighborhood, the original operators can be approximated by linear ones.

Assume that the neural operator $\mathcal{G}_\theta$ is Lipschitz continuous. This follows from the fact that it is a composition of Lipschitz functions with bounded parameters. Under the standing assumptions for the state equation, the operator $\mathcal{G}$ is also Lipschitz; that is, there exist constants $L, L_\theta > 0$ such that

$$\|\mathcal{G}(\mathbf{q}_1) - \mathcal{G}(\mathbf{q}_2)\|_2 \le L\|\mathbf{q}_1 - \mathbf{q}_2\|_2, \tag{10}$$

$$\|\mathcal{G}_\theta(\mathbf{q}_1) - \mathcal{G}_\theta(\mathbf{q}_2)\|_2 \le L_\theta\|\mathbf{q}_1 - \mathbf{q}_2\|_2, \tag{11}$$

for all controls $\mathbf{q}_1,\ \mathbf{q}_2 \in Q_{ad}$.

Suppose that $\mathcal{G}$ is Fréchet differentiable at $\mathbf{q}^{(k)}$ (which follows from the regularity of the flow problem under standard assumptions), and that the approximating neural operator $\mathcal{G}_\theta$ is differentiable at $\mathbf{q}_n^{(k)}$. Introduce the corresponding linear operators $\widetilde{\mathcal{G}}$ and $\widetilde{\mathcal{G}}_\theta$:

$$\widetilde{\mathcal{G}}(\mathbf{q}) := \mathcal{G}'(\mathbf{q}^{(k)})(\mathbf{q} - \mathbf{q}^{(k)}), \tag{12}$$

$$\widetilde{\mathcal{G}}_\theta(\mathbf{q}_n) := \mathcal{G}_\theta'(\mathbf{q}_n^{(k)})(\mathbf{q}_n - \mathbf{q}_n^{(k)}), \tag{13}$$

where $\mathcal{G}'(\mathbf{q}^{(k)})$ and $\mathcal{G}_\theta'(\mathbf{q}_n^{(k)})$ denote Fréchet derivatives.

The reduced functionals of the optimal control problem with these linearized operators read

$$\widetilde{J}(\mathbf{q}) = \frac{\beta}{2}\|\widetilde{\mathcal{G}}\mathbf{q}\|_2^2 + \frac{\lambda}{2}\|\Psi\widetilde{\mathcal{G}}\mathbf{q}\|_2^2 + \frac{1}{2}\|\mathbf{q} - \mathbf{q}_{\max}\|_2^2, \tag{14}$$

$$\widetilde{J}_n(\mathbf{q}_n) = \frac{\beta}{2}\|\widetilde{\mathcal{G}}_\theta\mathbf{q}_n\|_2^2 + \frac{\lambda}{2}\|\Psi\widetilde{\mathcal{G}}_\theta\mathbf{q}_n\|_2^2 + \frac{1}{2}\|\mathbf{q}_n - \mathbf{q}_{\max}\|_2^2 \tag{15}$$

We use $\|\cdot\|_2$ for the corresponding L^2 norms; the underlying space is clear from the argument. Operator norms between the respective Hilbert spaces are denoted by

$$\|A\|_2 = \sup_{\substack{x\in X\\ \|x\|_X \le 1}} \|Ax\|_Y.$$

Theorem 1. *Assume that conditions* (10)–(15) *hold, and that the neural operator $\widetilde{\mathcal{G}}_\theta$ approximates the solution operator $\widetilde{\mathcal{G}}$ with error $\|\widetilde{\mathcal{G}} - \widetilde{\mathcal{G}}_\theta\|_2 \le \varepsilon$. Then, for the optimal control problem the following upper bound in the L^2 norm holds:*

$$\|\mathbf{q}^* - \mathbf{q}_n^*\|_2 \le \frac{C\varepsilon(\beta+\lambda)\|\mathbf{q}_{\max}\|_2}{\alpha \cdot \alpha_\theta},$$

where $\beta \in \mathbb{R}_+$ is the regularization parameter, $\alpha_\theta = (\beta + \lambda d_{\min})\,\sigma_{\min}(\widetilde{\mathcal{G}}_\theta)^2 + 1$, $\alpha = (\beta + \lambda d_{\min})\,\sigma_{\min}(\widetilde{\mathcal{G}})^2 + 1$, $C = \|\widetilde{\mathcal{G}}\|_2 + \|\widetilde{\mathcal{G}}_\theta\|_2$, $\mathbf{q}_{\max}$ denotes the operational upper bounds on the controls.

Proof. Let $\mathbf{q}^*$ be the optimal control for $\widetilde{\mathcal{G}}$: $\mathbf{q}^* = \arg\min \widetilde{J}(\mathbf{q})$ and similarly, $\mathbf{q}_n^*$ for $\widetilde{\mathcal{G}}_\theta$: $\mathbf{q}_n^* = \arg\min \widetilde{J}_n(\mathbf{q})$. Then the first-order optimality conditions (Euler–Lagrange equations) for $\mathbf{q}^*$ (16) and $\mathbf{q}_n^*$ (17) are:

$$\widetilde{J}'(\mathbf{q}^*) = \beta\widetilde{\mathcal{G}}^\dagger\widetilde{\mathcal{G}}\mathbf{q}^* + \lambda\widetilde{\mathcal{G}}^\dagger\Psi\widetilde{\mathcal{G}}\mathbf{q}^* + \mathbf{q}^* - \mathbf{q}_{\max} = 0, \tag{16}$$

$$\widetilde{J}_\theta'(\mathbf{q}_n^*) = \beta\widetilde{\mathcal{G}}_\theta^\dagger\widetilde{\mathcal{G}}_\theta\mathbf{q}_n^* + \lambda\widetilde{\mathcal{G}}_\theta^\dagger\Psi\widetilde{\mathcal{G}}_\theta\mathbf{q}_n^* + \mathbf{q}_n^* - \mathbf{q}_{\max} = 0, \tag{17}$$

where $\widetilde{\mathcal{G}}^\dagger$, $\widetilde{\mathcal{G}}_\theta^\dagger$ and $\mathcal{S}^\dagger$ denote adjoint operators [Hinze, 2009].

Subtracting the second equation from the first yields

$$\beta(\widetilde{\mathcal{G}}^\dagger\widetilde{\mathcal{G}}\mathbf{q}^* - \widetilde{\mathcal{G}}_\theta^\dagger\widetilde{\mathcal{G}}_\theta\mathbf{q}_n^*) + \lambda(\widetilde{\mathcal{G}}^\dagger\Psi\widetilde{\mathcal{G}}\mathbf{q}^* - \widetilde{\mathcal{G}}_\theta^\dagger\Psi\widetilde{\mathcal{G}}_\theta\mathbf{q}_n^*) + (\mathbf{q}^* - \mathbf{q}_n^*) = 0.$$

Let $\delta\mathbf{q}_n = \mathbf{q}^* - \mathbf{q}_n^*$ denote the control error. Rearranging terms to isolate the operator acting on $\delta\mathbf{q}_n$, add and subtract $\beta\widetilde{\mathcal{G}}_\theta^\dagger\widetilde{\mathcal{G}}_\theta\mathbf{q}^*$ and $\lambda\widetilde{\mathcal{G}}_\theta^\dagger\Psi(\widetilde{\mathcal{G}}_\theta\mathbf{q}^*)$:

$$\Big(\beta\,\widetilde{\mathcal{G}}_\theta^\dagger\widetilde{\mathcal{G}}_\theta + I\Big)\delta\mathbf{q} + \lambda\,\widetilde{\mathcal{G}}_\theta^\dagger\big[\Psi(\widetilde{\mathcal{G}}_\theta\mathbf{q}^*) - \Psi(\widetilde{\mathcal{G}}_\theta\mathbf{q}_n^*)\big] = \beta\,(\widetilde{\mathcal{G}}_\theta^\dagger\widetilde{\mathcal{G}}_\theta - \widetilde{\mathcal{G}}^\dagger\widetilde{\mathcal{G}})\mathbf{q}^* + \lambda\,(\widetilde{\mathcal{G}}_\theta^\dagger\Psi(\widetilde{\mathcal{G}}_\theta\mathbf{q}^*) - \widetilde{\mathcal{G}}^\dagger\Psi(\widetilde{\mathcal{G}}\mathbf{q}^*)), \tag{18}$$

The threshold function $\psi(x) = [x - d_*]_+$ is convex, 1-Lipschitz, and differentiable almost everywhere with $\psi' \in \{0, 1\}$. For any $x, y \in \mathbb{R}$ one has $\psi(x) - \psi(y) = c(x, y)\,(x - y)$, with $c(x, y) \in [0, 1]$. elementwise in $m = 1, \dots, M_w$ and in time t, this yields a bounded diagonal (multiplication) operator D with $0 \preceq D \preceq I$ such that $\Psi(u) - \Psi(v) = D\,(u - v)$.

Thus, for $u = \widetilde{\mathcal{G}}_\theta\mathbf{q}^*$, $v = \widetilde{\mathcal{G}}_\theta\mathbf{q}_n^*$ we obtain: $\widetilde{\mathcal{G}}_\theta^\dagger\big[\Psi(\widetilde{\mathcal{G}}_\theta\mathbf{q}^*) - \Psi(\widetilde{\mathcal{G}}_\theta\mathbf{q}_n^*)\big] = \widetilde{\mathcal{G}}_\theta^\dagger D\,\widetilde{\mathcal{G}}_\theta\,\delta\mathbf{q}$. Substituting into (18) gives

$$\underbrace{\Big(\beta\,\widetilde{\mathcal{G}}_\theta^\dagger\widetilde{\mathcal{G}}_\theta + \lambda\,\widetilde{\mathcal{G}}_\theta^\dagger D\,\widetilde{\mathcal{G}}_\theta + I\Big)}_{=:\mathcal{H}_\theta}\,\delta\mathbf{q} = \beta\,(\widetilde{\mathcal{G}}_\theta^\dagger\widetilde{\mathcal{G}}_\theta - \widetilde{\mathcal{G}}^\dagger\widetilde{\mathcal{G}})\mathbf{q}^* + \lambda\,(\widetilde{\mathcal{G}}_\theta^\dagger\Psi(\widetilde{\mathcal{G}}_\theta\mathbf{q}^*) - \widetilde{\mathcal{G}}^\dagger\Psi(\widetilde{\mathcal{G}}\mathbf{q}^*)). \tag{19}$$

The quadratic form on the left-hand side of (19) is the Hessian operator $\mathcal{H}_\theta$ of the reduced functional $\widetilde{J}_n$. The operator is self-adjoint, positive definite, and coercive. In particular,

$$\begin{aligned}\langle\mathcal{H}_\theta\mathbf{q}_n,\ \mathbf{q}_n\rangle &= \beta\|\widetilde{\mathcal{G}}_\theta\mathbf{q}_n\|_2^2 + \lambda d_{\min}\,\|\widetilde{\mathcal{G}}_\theta\mathbf{q}_n\|_2^2 + \|\mathbf{q}_n\|_2^2\\ &= (\beta + \lambda d_{\min})\|\widetilde{\mathcal{G}}_\theta\mathbf{q}_n\|_2^2 + \|\mathbf{q}_n\|_2^2\\ &\ge \alpha_\theta\|\mathbf{q}_n\|_2^2 \quad \forall\mathbf{q}_n \ne 0.\end{aligned} \tag{20}$$

Here $\alpha_\theta > 0$ is the coercivity constant of $\mathcal{H}_\theta$, and $d_{\min} \in [0, 1]$ is the minimal diagonal entry of D.

Express the control error via the inverse operator $\mathcal{H}_\theta^{-1}$:

$$\delta \mathbf{q}_n = \mathcal{H}_\theta^{-1}\Big[\beta\,(\widetilde{\mathcal{G}}_\theta^\dagger \widetilde{\mathcal{G}}_\theta - \widetilde{\mathcal{G}}^\dagger \widetilde{\mathcal{G}})\mathbf{q}^* + \lambda\,(\widetilde{\mathcal{G}}_\theta^\dagger \Psi(\widetilde{\mathcal{G}}_\theta \mathbf{q}^*) - \widetilde{\mathcal{G}}^\dagger \Psi(\widetilde{\mathcal{G}}\mathbf{q}^*))\Big]. \tag{21}$$

Taking norms on both sides of (21) yields

$$\|\mathbf{q}^* - \mathbf{q}_n^*\|_2 \le \|\mathcal{H}_\theta^{-1}\|_2 \cdot \Big[\beta \underbrace{\|(\widetilde{\mathcal{G}}_\theta^\dagger \widetilde{\mathcal{G}}_\theta - \widetilde{\mathcal{G}}^\dagger \widetilde{\mathcal{G}})\mathbf{q}^*\|_2}_{(\mathbf{I})} + \lambda \underbrace{\|\widetilde{\mathcal{G}}_\theta^\dagger \Psi(\widetilde{\mathcal{G}}_\theta \mathbf{q}^*) - \widetilde{\mathcal{G}}^\dagger \Psi(\widetilde{\mathcal{G}}\mathbf{q}^*)\|_2}_{(\mathbf{II})}\Big].$$

We now bound the right-hand side (the error source):

$$\begin{aligned}(\mathbf{I}) &= \|(\widetilde{\mathcal{G}}_\theta^\dagger(\widetilde{\mathcal{G}}_\theta - \widetilde{\mathcal{G}}) + (\widetilde{\mathcal{G}}_\theta^\dagger - \widetilde{\mathcal{G}}^\dagger)\widetilde{\mathcal{G}})\mathbf{q}^*\|_2 \\ &\le \Big(\|\widetilde{\mathcal{G}}_\theta\|_2\|\widetilde{\mathcal{G}}_\theta - \widetilde{\mathcal{G}}\|_2 + \|\widetilde{\mathcal{G}}_\theta - \widetilde{\mathcal{G}}\|_2\|\widetilde{\mathcal{G}}\|_2\Big)\|\mathbf{q}^*\|_2 \\ &= (\|\widetilde{\mathcal{G}}_\theta\|_2 + \|\widetilde{\mathcal{G}}\|_2)\|\mathbf{q}^*\|_2\|\widetilde{\mathcal{G}}_\theta - \widetilde{\mathcal{G}}\|_2.\end{aligned}$$

By Lipschitz continuity of $\widetilde{\mathcal{G}}_\theta$ and $\widetilde{\mathcal{G}}$, we obtain

$$\|(\widetilde{\mathcal{G}}_\theta^\dagger \widetilde{\mathcal{G}}_\theta - \widetilde{\mathcal{G}}^\dagger \widetilde{\mathcal{G}})\mathbf{q}^*\|_2 \le C\|\mathbf{q}^*\|_2\|\widetilde{\mathcal{G}}_\theta - \widetilde{\mathcal{G}}\|_2.$$

Here $C = \|\widetilde{\mathcal{G}}\|_2 + \|\widetilde{\mathcal{G}}_\theta\|_2$.

For $(\mathbf{II})$ (using that Ψ is 1-Lipschitz and $\|\Psi(u)\| \le \|u\|$ elementwise) , add and subtract $\widetilde{G}^\dagger \Psi(\widetilde{G}_\theta \mathbf{q}^*)$:

$$\begin{aligned}(\mathbf{II}) &= \big(\widetilde{\mathcal{G}}_\theta^\dagger - \widetilde{G}^\dagger\big)\Psi(\widetilde{G}_\theta \mathbf{q}^*) + \widetilde{G}^\dagger\big(\Psi(\widetilde{G}_\theta \mathbf{q}^*) - \Psi(\widetilde{\mathcal{G}}\mathbf{q}^*)\big) \\ &\le \|\widetilde{\mathcal{G}}_\theta^\dagger - \widetilde{G}^\dagger\|_2\|\Psi(\widetilde{\mathcal{G}}_\theta \mathbf{q}^*)\|_2 \\ &+ \|\widetilde{\mathcal{G}}^\dagger\|_2\|\Psi(\widetilde{\mathcal{G}}_\theta \mathbf{q}^*) - \Psi(\widetilde{\mathcal{G}}\mathbf{q}^*)\|_2 \\ &\le C\|\mathbf{q}^*\|_2\|\widetilde{\mathcal{G}}_\theta - \widetilde{\mathcal{G}}\|_2.\end{aligned} \tag{22}$$

To bound $\mathbf{q}^*$, note from (16) that $\mathcal{H}\mathbf{q}^* = \mathbf{q}_{\max}$, hence $\mathbf{q}^* = \mathcal{H}^{-1}\mathbf{q}_{\max}$. Let $\alpha > 0$ denote the coercivity constant of the operator $\mathcal{H}$ then $\|\mathcal{H}^{-1}\|_2 \le 1/\alpha$. Therefore, the estimate of the norm $\|\mathbf{q}^*\|_2$ has the form

$$\|\mathbf{q}^*\|_2 \le \alpha^{-1}\,\|\mathbf{q}_{\max}\|_2.$$

From (20), we similarly obtain $\|\mathcal{H}_\theta^{-1}\|_2 \le 1/\alpha_\theta$. Substituting the obtained estimates into the inequality for $\|\mathbf{q}^* - \mathbf{q}_n^*\|_2$ and using $\|\widetilde{\mathcal{G}}_\theta - \widetilde{\mathcal{G}}\|_2 \le \varepsilon$ yields

$$\|\mathbf{q}^* - \mathbf{q}_n^*\|_2 \le \frac{C\varepsilon(\beta+\lambda)\|\mathbf{q}_{\max}\|_2}{\alpha \cdot \alpha_\theta}. \tag{23}$$

$\square$

Here $\alpha_\theta = (\beta + \lambda d_{\min})\,\sigma_{\min}(\widetilde{\mathcal{G}}_\theta)^2 + 1$, $\alpha = (\beta + \lambda d_{\min})\,\sigma_{\min}(\widetilde{\mathcal{G}})^2 + 1$.

The obtained estimate shows that the discrepancy between the exact and surrogate-based optimal controls grows proportionally to the approximation error ε, while its dependence on the Lipschitz characteristics of $\widetilde{\mathcal{G}}_\theta$ captures how the surrogate's dynamical sensitivity affects error propagation.

5 Numerical experiments

This section presents numerical experiments illustrating the effect of the regularization parameter $\beta \in [0, 2]$ on the trade-off between the magnitude of well rates and pressure drawdown. We consider two regimes: with a threshold penalty ($\lambda = 5$) and without it ($\lambda = 0$). The trained neural operator $\mathcal{G}_\theta$ is used for the forward evaluations. Controls were updated by projected gradient method onto the admissible set $Q_{ad} = \{\mathbf{q} : 0 \le q_m(t) \le q_{m,\max}(t)\}$. After each gradient step, the projection $\mathrm{Proj}_{Q_{ad}}$ is applied elementwise, clipping each component of the control vector to its admissible interval. This ensures that the iterative optimization remains physically consistent, preventing negative production rates and prohibiting values exceeding operational constraints.

The analysis criteria are defined by the norms of the reduced objective terms: $J_1(\mathbf{q}) := \|\mathbf{q} - \mathbf{q}_{\max}\|_2$, $J_2(\mathbf{q}) := \|\Delta \mathbf{p}\|_2$. The results are shown in Figures 1–4.

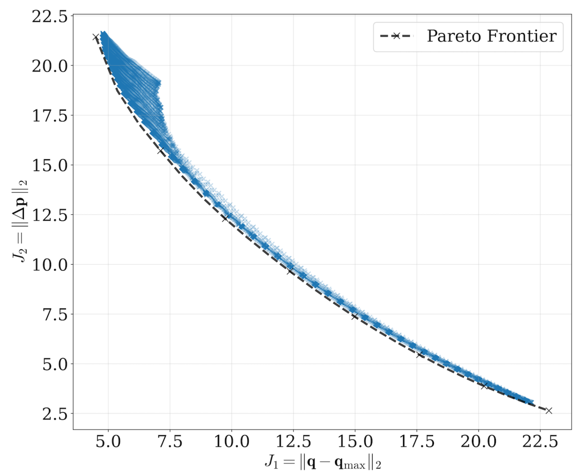

Figure 1. Set of solutions for $\lambda = 5$.

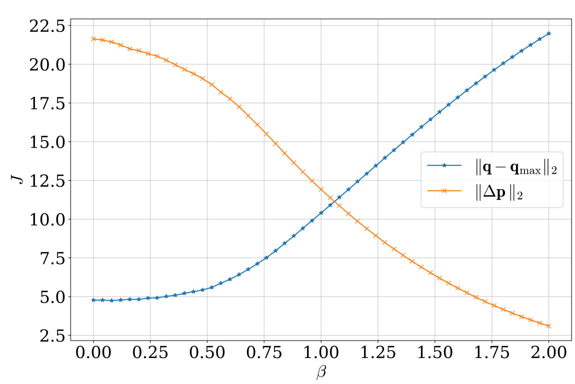

Figure 2. Dependence of functional terms on β for $\lambda = 5$.

Note that for values of J_1 close to the boundary, different levels of J_2 are attainable; that is, with a slight deviation from the operational maxima one can achieve more or less favorable drawdown levels (Figure 2).

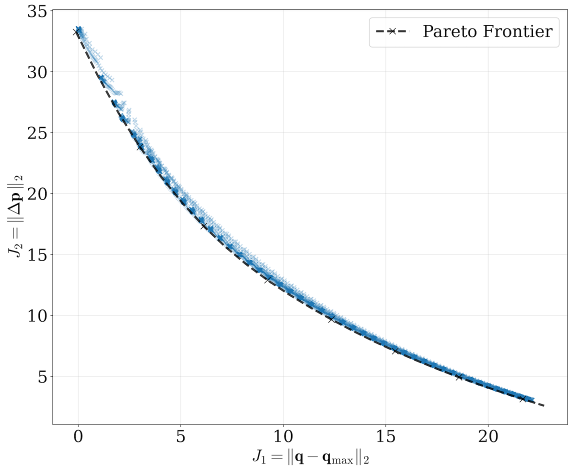

Figure 3. Set of solutions for $\lambda = 0$.

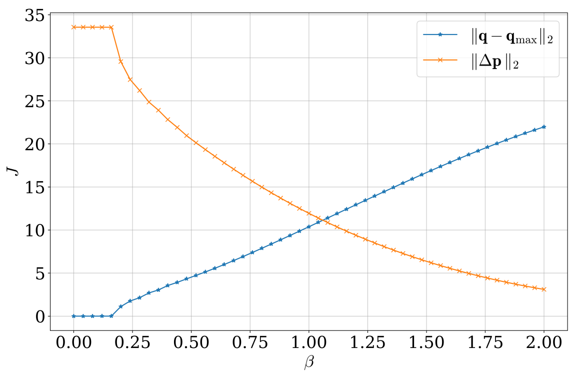

Figure 4. Dependence of functional terms on β for $\lambda = 0$.

In the absence of a threshold penalty for exceeding the pressure drawdown limit (i.e., $\lambda = 0$), the set of points (J_1, J_2) forms a smooth and monotonic trade-off curve (Figure 3), without any pronounced vertical segments. For small regularization values, $\beta \leq 0.2$, the optimal solutions collapse to the maximal-rate control, $\mathbf{q}^* = \mathbf{q}_{\max}$ (so $J_1 = 0$). As β increases beyond this range, the control vector gradually deviates from $\mathbf{q}_{\max}$, resulting in a monotonic increase in J_1 and a simultaneous decrease in drawdown, reflected by lower values of J_2.

Note that the optimal control solution is computed in approximately one minute on a single NVIDIA Tesla T4, a performance not achievable with conventional simulation-based approaches.

6 Conclusion

We proposed a PDE-constrained optimal control framework for subsurface reservoir systems that replaces expensive forward solves with trained neural operator surrogates while retaining gradient access via automatic differentiation. We established an a priori L^2 bound on the control error that links performance to the surrogate's operator-norm approximation error and the coercivity of the reduced Hessian. Numerical experiments confirm a controllable trade-off between adherence to operational rate targets and pressure-drawdown reduction, alongside substantial computational efficiency. These results indicate that neural operator surrogates enable fast, reliable well-control optimization and decision support in reservoir engineering.

References

Antil, H., Kouri, D. P., Lacasse, M.-D., and Ridzal, D., editors (2018). *Frontiers in PDE-Constrained Optimization*, vol. 163 of *The IMA Volumes in Mathematics and Its Applications*. Springer New York, New York, NY.

Arguchintsev, A. and Kopylov, D. (2023). Numerical solution of the initial-boundary value problem describing separation processes in a distillation column. *Cybernetics and Physics*, **12** (3), pp. 169–173.

Arguchintsev, A. and Kopylov, D. (2024). Numerical optimization of separation processes in a distillation column. *Cybernetics and Physics*, **13** (3), pp. 241–247.

Aziz, K. and Settari, A. (1979). *Petroleum Reservoir Simulation*. Applied science publ, London New York.

Chen, Z. (2007). *Reservoir Simulation: Mathematical Techniques in Oil Recovery*. Society for Industrial and Applied Mathematics.

Ertekin, T., Abou-Kassem, J. H., and King, G. R. (2001). *Basic Applied Reservoir Simulation*. Number v. 7 in SPE Textbook Series. Society of Petroleum Engineers, Richardson, Tex.

Hinze, M. (2009). *Optimization with PDE Constraints*. Number v. 23 in Mathematical Modelling–Theory and Applications. Springer, Dordrecht.

Istomin, V. A. and Pavlov, S. A. (2023). Suitability of different machine learning methods for high-speed flow modeling issues. *Cybernetics and Physics*, **12** (4), pp. 264–274.

Jansen, J. (2011). Adjoint-based optimization of multiphase flow through porous media – A review. *Computers & Fluids*, **46** (1), pp. 40–51.

Kourounis, D., Durlofsky, L. J., Jansen, J. D., and Aziz, K. (2014). Adjoint formulation and constraint handling for gradient-based optimization of compositional reservoir flow. *Computational Geosciences*, **18** (2), pp. 117–137.

Kovachki, N., Li, Z., Liu, B., Azizzadenesheli, K., Bhattacharya, K., Stuart, A., and Anandkumar, A. (2023).

Neural Operator: Learning Maps Between Function Spaces With Applications to PDEs. *The Journal of Machine Learning Research*, **24** (89), pp. 1–97.

Li, Z., Kovachki, N., Azizzadenesheli, K., Liu, B., Bhattacharya, K., Stuart, A., and Anandkumar, A. (2020). Fourier Neural Operator for Parametric Partial Differential Equations.

Lions, J. (1971). *Optimal Control of Systems Governed by Partial Differential Equations:*. Grundlehren Der Mathematischen Wissenschaften in Einzeldarstellungen Mit Besonderer Berücksichtigung Der Anwendungsgebiete. Springer-Verlag.

Lu, L., Jin, P., Pang, G., Zhang, Z., and Karniadakis, G. E. (2021). Learning nonlinear operators via DeepONet based on the universal approximation theorem of operators. *Nature Machine Intelligence*, **3** (3), pp. 218–229.

Lurie, K. A. (1993). *Applied Optimal Control Theory of Distributed Systems*. Springer US, Boston, MA.

Oleĭnik, O. A., Kalashnikov, A. S., and Zhou, Y.-l. (1958). The Cauchy problem and boundary problems for equations of the type of non-stationary filtration. *Izv. Akad. Nauk SSSR, Ser. Mat.*, **22**, pp. 667–704.

Sarma, P., Durlofsky, L. J., Aziz, K., and Chen, W. H. (2006). Efficient real-time reservoir management using adjoint-based optimal control and model updating. *Computational Geosciences*, **10** (1), pp. 3–36.

Sirota, D. D., Gushchin, K. A., Khan, S. A., Kostikov, S. L., and Butov, K. A. (2024). Neural Operators for Hydrodynamic Modeling of Underground Gas Storages. *Moscow University Physics Bulletin*, **79** (S2), pp. S922–S934.

Sirota, D. D., Khan, S. A., Kostikov, S. L., and Butov, K. A. (2025). Neural operators for mathematical modeling of transient fluid flow in subsurface reservoir systems. *Vestnik of Saint Petersburg University. Applied Mathematics. Computer Science. Control Processes*, **21** (3), pp. 385–400.

Vazquez, J. L. (2006). *The Porous Medium Equation: Mathematical Theory*. Oxford University PressOxford, 1 edition.

Zakirov, I., I. Aanonsen, S., S. Zakirov, E., and M. Palatnik, B. (1996). Optimizing Reservoir Performance by Automatic Allocation of Well Rates. In *ECMOR V - 5th European Conference on the Mathematics of Oil Recovery*, Leoben, Austria,, European Association of Geoscientists & Engineers.